NATIONAL UNIVERSITY OF SCIENCE AND TECHNOLOGY POLITEHNICA BUCHAREST

DOCTORAL SCHOOL OF ELECTRICAL ENGINEERING

DOCTORAL THESIS

-SUMMARY-

CONTRIBUTIONS TO THE DEVELOPMENT OF A HYBRID POWER SUPPLY SYSTEM WITH RENEWABLE ENERGY SOURCES

PhD coordinator:

Prof.univ.dr.ing. Mihai Octavian POPESCU

PhD student:

Ing. Ciprian POPA

Bucharest
2025

CONTENTS

CHAPTER 1 - INTRODUCTION

1.1. PROBLEM STATEMENT

The research explores the efficient integration of wind and solar energy into a hybrid power supply system, aiming to develop a sustainable and optimized solution for current energy demands. The study focuses on two main directions:

- *Energy management in a hybrid system*. This aspect involves coordinating the energy generated by wind turbines and photovoltaic panels to ensure uninterrupted power supply to consumers despite environmental variability. Chapter 5 addresses the design of the hybrid system using compatible technological components, advanced controllers, and inverters. The implemented solutions aim to minimize losses, maximize efficiency, and resolve encountered issues, such as equipment limitations or connection challenges.
- *Experimental validation of mathematical models*. Experiments compared the simulation results obtained in Matlab (Simulink) with practical data from hybrid system testing. In Chapter 4, mathematical models and detailed block diagrams were developed for each renewable source and the integrated system, analyzing their interactions and performance under varied operating conditions. This process enabled a comprehensive assessment of the system's efficiency and adaptability..

By integrating renewable energy sources and optimizing energy flows, the research contributes to the development of a sustainable hybrid system capable of meeting current energy needs and adapting to changing environmental conditions.

1.2. RESEARCH OBJECTIVES

This research aims to develop, optimize, and validate a hybrid power system based on renewable energy sources, combining wind turbines and photovoltaic panels. The objectives of the study are detailed and aim to fulfill essential directions for optimizing and implementing an efficient and sustainable system. Therefore, the doctoral thesis seeks to pursue the following:

1. *Literature review* - Identifying technological advancements and analyzing the components of hybrid systems (turbines, photovoltaic panels, battery storage, inverters, controllers) for optimal energy management.
2. *Development of mathematical models* - Creating and simulating mathematical models in Matlab (Simulink), considering meteorological factors and the variables of a fluctuating environment to optimize energy performance. Experimental validation of the model through comparison with simulation results and the development of an original mathematical model capable of analyzing the influence of environmental factors on energy production.
3. *Implementation and experimental testing* - Constructing a functional prototype and developing an autonomous wind-photovoltaic hybrid system, tested under real-world conditions to calibrate and validate the mathematical models, demonstrating the system's efficiency and applicability.

This study makes a significant contribution to the optimization of hybrid systems, improving the anticipation and management of energy production based on external conditions.

1.3. STRUCTURE AND CONTENT OF THE THESIS

The doctoral thesis is structured into six chapters that focus on the development, simulation, and validation of a wind-photovoltaic hybrid system based on renewable energy sources..

Chapter 1 - Introduction, contextualizes the research by highlighting the importance of renewable energy sources and the thesis objectives.

Chapter 2 - Current state of development, analyzes advancements in renewable energy, with a focus on wind turbines and photovoltaic panels.

Chapter 3 - Fundamental Principles, covers the fundamentals of hybrid systems, including components such as wind turbines, photovoltaic panels, battery storage, inverters, and controllers. The analysis is based on over 100 articles from international databases.

Chapter 4 - Mathematical models and performance simulation of hybrid systems, presents mathematical algorithms for estimating energy production, simulated in Matlab (Simulink), along with an original model for system performance analysis.

Chapter 5 - Experimental implementation and contributions to performance optimization of hybrid systems, describes the design and testing of the hybrid system prototype, validating experimental results against simulated data..

Chapter 6 - Conclusions and development perspectives, summarizes the main original contributions and proposes future research directions..

This research makes significant theoretical and practical contributions, validating the utility and efficiency of hybrid systems under diverse environmental conditions.

CHAPTER 2 - CURRENT STATE OF RENEWABLE ENERGY SOURCES

2.1. TECHNOLOGICAL CONCEPTS OF WIND TURBINES

Bladeless wind turbine systems

Bladeless wind turbines utilize aeroelastic resonance to convert wind energy into electricity, offering advantages such as lower costs, the absence of rotating components, and operation at low wind speeds. However, their efficiency varies with wind speed, prompting research into solutions like magnetorheological elastomers for resonance adjustment, thus contributing to more sustainable and eco-friendly energy solutions [1], [2], [3], [4], [5], [6], [7].

Passive wind turbine systems

Passive wind turbine technology is based on the Venturi effect. When a fluid flows through a constricted section formed between two optimally configured profiles, a pressure drop occurs, drawing air from the edges of the channel. By placing a small rotor in this setup, wind energy is captured, providing a silent, low-maintenance, environmentally friendly system that is efficient in generating electricity [8], [9], [10], [11], [12].

Modular multi-rotor wind system

The modular multi-rotor wind system is based on an innovative design that integrates smaller turbines into a vertical structure. This arrangement optimizes energy capture from wind flows by eliminating active yaw mechanisms and reducing dependency on directional fluctuations, offering an efficient and cost-effective alternative to large conventional turbines [13], [14], [15], [16], [17].

2.2. TECHNOLOGICAL CONCEPTS OF PHOTOVOLTAIC PANELS

Bifacial photovoltaic systems

Bifacial photovoltaic systems, equipped with solar cells on both sides and a transparent layer, capture both direct and diffuse or reflected light, generating up to 35-40% more energy compared to monofacial panels, especially when integrated with solar tracking mechanisms [18], [19], [20], [21], [22], [23], [24], [25].

Transparent photovoltaic panels

Transparent photovoltaic panels, with extensive applications in agriculture and urban buildings, combine efficient energy generation with crop protection and optimal storage of agricultural products. Agrivoltaic systems further enhance biomass and energy production on the same surface. Using transparent luminescent solar concentrator technology, these panels achieve an efficiency of 10.8% and a transparency of 45.8%, maximizing the conversion of ultraviolet and infrared radiation [26], [27], [28], [29], [30].

The technology behind transparent solar panels represents a major innovation in renewable energy, allowing integration into the glass surfaces of buildings to generate electricity from the solar spectrum without compromising natural lighting. This contributes to energy efficiency, reduced cooling costs, and the development of sustainable infrastructures compatible with various architectural designs [27], [29], [30].

CHAPTER 3 - FUNDAMENTAL PRINCIPLES OF RENEWABLE ENERGY SOURCES

Throughout history, energy has been a central element in the development of humanity. However, the excessive dependence on fossil fuels such as coal, oil, and natural gas has led to adverse effects, including global warming and climate change. Traditional resources are finite, and the transition to renewable sources, such as solar, wind, hydroelectric, and geothermal energy, is becoming essential, requiring research to improve their efficiency, costs, and stability [31], [32], [33].

Renewable energy, derived from self-regenerating sources such as the sun, wind, water, and biomass, is used to produce electricity, fuels, and heat, offering advantages such as low environmental impact and virtually unlimited potential. Although sources such as hydroelectric, wind, and solar energy are among the most widely used globally, they face challenges such as intermittency and unpredictability, which affect the efficient operation of energy systems and their economic feasibility [34], [35].

In the last two decades, the capacity of renewable energy sources has grown significantly, with notable growth rates in wind and solar energy [36], [37].

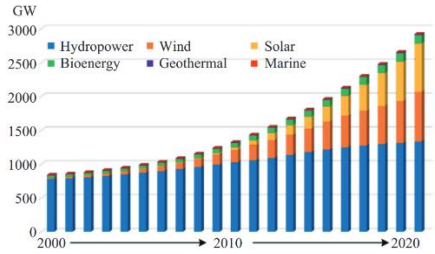

Fig. 0.1. Cumulative global capacity of renewable energy sources from 2000-2020 based on IRENA available data [36], [37]

3.1. WIND TURBINE TECHNOLOGY

Wind energy has evolved significantly since 2013, from small turbines to multi-megawatt turbines, which are now widely integrated into electrical grids and wind farms. Although wind turbines are becoming increasingly efficient, research continues to optimize their performance and costs by implementing new generators and control technologies for more efficient integration into electrical grids [38], [39], [40], [41].

Modern turbines utilize the principle of aerodynamic lift and can be classified into two types: horizontal-axis or vertical-axis (aerodynamic resistance), with various control systems designed to maximize energy production depending on wind speed. However, under varying wind conditions, turbines do not always operate at maximum power, and controlling the rotational speed or blade angle is essential for optimizing production [42], [43], [44].

Fig. 0.2. Classification of turbines based on the turbine axis position

Electricity generation through wind turbines offers significant benefits, such as the elimination of polluting emissions and low operational costs, with no waste production. Vertical-axis wind turbines are omnidirectional and have advantages such as lower installation heights and easier maintenance. However, they are less efficient compared to horizontal-axis turbines, which, although more complex, provide higher yields and are preferred in modern wind energy applications [42], [43], [45], [46], [47].

Disadvantages of wind turbines include noise and visual pollution, as well as the instability of energy production due to variable wind. However, technological advances have significantly reduced noise, and further development may expand their use in areas with limited wind potential [45].

Wind turbines capture wind energy through a rotor that is constantly adjusted to align perpendicular to the wind direction, converting the kinetic energy of the wind into mechanical energy. The rotor's movement is generated by the pressure difference between the exposed and opposite sides of the blades, and the mechanical energy is transformed into electrical energy through a generator. In the medium wind speed range, the system optimizes conversion efficiency by controlling the blade pitch angle and rotational speed to maintain an optimal power coefficient and control the generator's torque [45], [48], [49].

The wind energy conversion system consists of three major components: mechanical, electrical, and control, and is structured into three main stages: transforming the kinetic energy of the wind into mechanical energy, converting mechanical energy into electricity through the generator, and connecting to the electrical grid through a power converter. The key components for this conversion are the rotor, gearbox (in direct drive solutions), electric generator, power converter, and transformer [50], [51], [52].

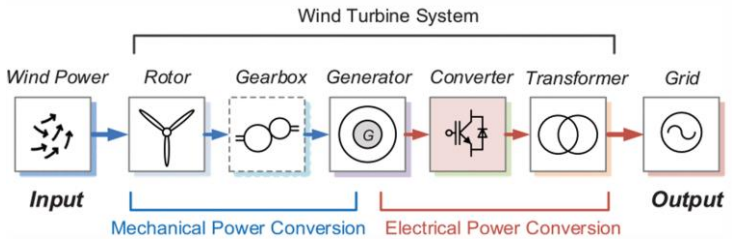

Fig. 0.3. Typical power conversion stages in a horizontal-axis wind turbine [52]

The main components of a horizontal-axis turbine are (Fig. 3.5.): 1. Blade 2. Blade support 3. Pitch angle control device 4. Hub 5. Rotor housing 6. Main support 7. Main shaft 8. Aircraft warning lights 9. Gearbox 10. Mechanical brakes 11. Hydraulic cooling devices 12. Generator 13. Power converter and electrical control, protection, and disconnect devices 14. Transformer 15. Anemometer 16. Nacelle frame 17. Support tower 18. Yaw system [53].

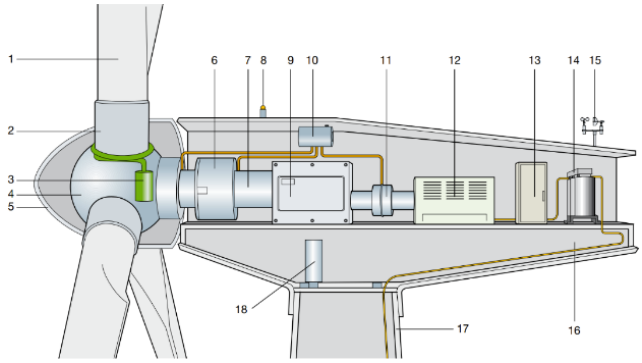

Fig. 0.4. Main components of a horizontal-axis wind turbine [53]

3.2. PHOTOVOLTAIC TECHNOLOGY

Renewable energy sources are considered a technological option for generating clean energy. One of these systems that has attracted particular interest is the photovoltaic system, regarded as one of the most promising renewable energy sources [89]. The photovoltaic energy system is increasingly attracting attention due to the use of non-polluting, renewable, and free solar energy, alongside growing concerns about environmental issues and the global energy crisis [54], [55], [56], [57].

The principle of operation of solar cells (Fig. 3.10.), is based on the photovoltaic effect, which involves the combination of two semiconductor materials, n-type and p-type, creating a potential difference. Photons from solar radiation transfer energy to electrons, releasing them from the crystalline lattice. This potential difference causes an organized flow of photo-generated carriers (electrons and holes), and through the contacts in the cell, an external circuit is formed that allows the circulation of electric current to provide useful energy [58].

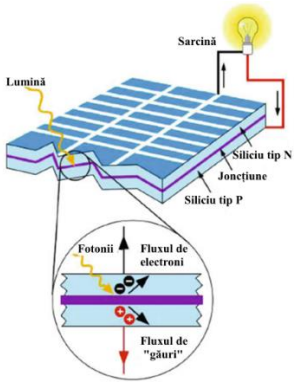

Fig. 0.5. Principle of operation of the solar cell [58]

The photovoltaic system consists of four main blocks: the power source, the DC-DC converter, the load, and the controller. The role of the static power converter is to adjust the impedance to ensure the maximum energy delivery from the panel. The photovoltaic module has a nonlinear power-voltage characteristic with a peak point (the maximum power point tracking–MPPT) where the system operates at maximum efficiency, and the intensity of solar radiation determines the variability of the generated power. The MPPT technique, combined with a DC-DC converter, optimizes the power extracted from the photovoltaic system, thereby maximizing the panel efficiency under changing weather conditions [59], [60], [61].

3.3. ENERGY STORAGE TECHNOLOGY

Energy storage has become an essential component in the development of smart energy systems, attracting the attention of international organizations and countries that have developed strategies for its implementation. Recent storage technologies offer a solution to address the intermittency of wind and photovoltaic energy, which are influenced by weather conditions, and power fluctuations can affect the frequency and voltage of the grid. By integrating energy storage systems into renewable energy production, power fluctuations can be reduced, maintaining system stability and minimizing the impact on the grid [62], [63], [64], [65], [66], [67], [68], [69], [70].

Energy storage technology involves transforming energy from one form to another so that it can be stored for later use. Energy may be stored in various media and then converted back into electrical energy when needed.

3.4. STUDIES ON HYBRID ENERGY GENERATION SYSTEMS

Solar and wind energy are widely used renewable sources, but due to the variability imposed by factors such as season, geography, and climate, they present high uncertainty, which can lead to energy instability. Combining the two sources using a DC-AC hybrid system allows complementary energy generation, improving reliability and reducing dependence on a single source. In isolated systems, the issue of excess energy must be managed, but this can affect system performance [71], [72], [73], [74], [75].

The hybrid system mainly consists of the following components: a photovoltaic energy generator, a wind energy generator, a controller, storage batteries, and an inverter, with the system structure presented in Fig. 3.6. [71], [76].

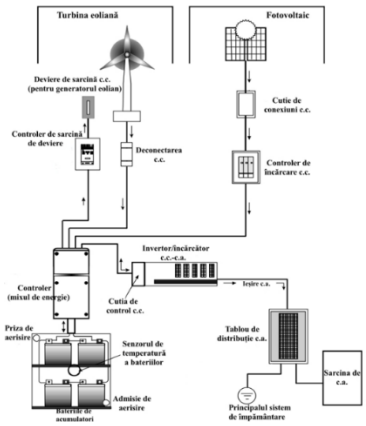

Fig. 0.6. Schematic diagram of an autonomous wind-photovoltaic hybrid system [76]

Photovoltaic energy results in the production of direct current from solar radiation, while wind energy comes from the kinetic energy of the wind, which often produces electricity in the form of alternating current. By combining the two energy sources, we can achieve not only maximum power but also an optimal system and better productivity that suits our needs [77], [78].

The total capacity of a wind-photovoltaic hybrid system is determined based on the estimated annual power demand, average wind speed, and solar radiation. Each renewable energy source is defined based on actual environmental conditions. To improve the performance of a hybrid system in various operating and environmental conditions, the maximum power point tracking of the photovoltaic system and the pitch control of the turbine blades are considered [79]. The hybrid system is chosen because the use of two connected sources has a more efficient rate than conventional systems based on a single renewable energy source [80].

There are two main objectives in designing the control strategy for hybrid renewable energy systems. One important issue is maximizing energy extraction since these energy sources provide varying amounts of power to the supply system under different conditions [81]. The photovoltaic panel and wind turbine offer highly fluctuating energy, heavily dependent on weather conditions. To overcome these issues, energy efficiency can be monitored by MPPT algorithms [82]. The other issue is regulating the output voltage around a predetermined value; in this case, the output voltage of the DC-AC converter must be controlled so that the DC-AC inverter delivers the appropriate voltage on the AC side [81]. Therefore, it is essential to provide solutions for a continuous and reliable energy source in remote areas. Hybrid power systems have proven to be a viable option [83].

CHAPTER 4 - MATHEMATICAL MODELS AND PERFORMANCE SIMULATION OF HYBRID SYSTEMS IN SIMULINK

4.1. HORIZONTAL AXIS WIND TURBINE

4.1.1. Mathematical models of the wind energy conversion system

Electricity generation through wind turbines is the result of the interaction between the wind and the rotor blades, a process in which the kinetic energy of the wind is converted into rotational mechanical energy, which is then transformed into electrical energy [53].

To determine the kinetic energy of an air flow moving with speed, v_1 (m/s), the following formula can be used [53], [84], [85]:

$$E_c = \frac{m \cdot v_1^2}{2} \tag{4.1}$$

Therefore, the specific available power, $P_{available}$ of a mass of air is [53], [85]:

$$P_{available} = \frac{dE_c}{dt} = \frac{\mathrm{q} \cdot v_1^2}{2} \tag{4.2}$$

The capacity can be expressed by the formula:

$$q = \frac{dm}{dt} = m = \rho \cdot \mathrm{S} \cdot v_1 \tag{4.3}$$

, this is known as the continuity equation, where m is the moving air mass (kg/s), influenced by the air density ρ and the volume that passes through a surface area S (m^2) of the air stream's cross-section considered [53], [84], [85].

The air density varies depending on pressure and temperature [42], according to the ideal gas law. Since pressure and temperature change with altitude at the installation site, their combination affects the air density, which can be derived from the simplified relation (valid up to an altitude of 6000m) [53]:

$$\rho = \rho_0 - 1.194 \cdot 10^{-4} \cdot h \tag{4.4}$$

where ρ_0, represents the standard air density at sea level (kg/m^3), and h este is the height of the turbine tower above sea level [53].

With the necessary information about density, exposed surface area, and velocity, the available specific power of the air flow can be calculated in Watts [53], [84], [85]:

$$P_{available} = \frac{\rho S v_1^3}{2} \tag{4.5}$$

A simplified model, developed by Albert Betz, is often used to calculate the energy production of an ideal wind turbine, with the available incident power described by formula (4.5). The more kinetic energy the turbine can extract from the wind, the lower the wind speed will be at the turbine's exit.

The power coefficient C_p (or efficiency coefficient) is the ratio of the extracted power to the available wind power. This coefficient is also known as the "Betz limit," referring to the fundamental concept: "The maximum power that can theoretically be extracted from the airflow using an ideal turbine cannot exceed 59% of the available incident wind power."

To determine the performance coefficient of the turbine, C_p, a generic equation is used [53], [85]:

$$C_p(\lambda, \beta) = c_1 \left(\frac{c_2}{\lambda_i} - c_3 \beta - c_4 \right) e^{\frac{-c_5}{\lambda_i}} + c_6 \lambda \tag{4.6}$$

where,

$$\frac{1}{\lambda_i} = \frac{1}{\lambda + 0{,}08\beta} - \frac{0{,}035}{\beta^3 + 1} \tag{4.7}$$

The coefficients c_1 through c_6 are: $c_1 = 0.5176$, $c_2 = 116$, $c_3 = 0.4$, $c_4 = 5$, $c_5 = 21$ și $c_6 = 0.0068$. The maximum value of C_p is reached for $\beta = 0$, where β is the blade pitch angle [85], [86].

The aerodynamic characteristics of a blade are usually defined by the relationship between tip speed and power coefficient. The tip speed ratio, denoted by parameter λ, is the ratio between the tangential speed of the blade tips and the wind speed at the inlet of the air flow tube [53], [85], [86]:

$$\lambda = \frac{v_t}{v_1} = \frac{\omega_r \cdot R}{v_1} \tag{4.8}$$

$$\omega_r = \frac{2\Pi n}{60} \tag{4.9}$$

where ω_r, is the angular rotational speed of the rotor [rad/s], R is the radius of the rotor [m], and n is the rotor speed [rpm].

Since the power generated by a wind turbine depends on the power coefficient C_p and the available wind power, it can be expressed as [53]:

$$P = C_p \cdot \frac{\rho S v_1^3}{2} \tag{4.10}$$

The mechanical power generated can be calculated as follows [53]:

$$P_m = \eta_m \cdot C_p \cdot \frac{\rho S v_1^3}{2} \tag{4.11}$$

The electrical power generated can be calculated as follows [53]:

$$P_e = \eta_e \cdot \eta_m \cdot C_p \cdot \frac{\rho S v_1^3}{2} \tag{4.12}$$

The useful electrical power generated can be calculated as follows [53]:

$$P_u = \eta_{aux} \cdot \eta_e \cdot \eta_m \cdot C_p \cdot \frac{\rho S v_1^3}{2} \tag{4.13}$$

where [53]:

- η_m is the overall mechanical efficiency of the transmission system;
- η_e is the generator efficiency;
- η_{aux} is the auxiliary circuit efficiency.

The horizontal-axis wind turbine, through which experimental data is to be collected, includes fixed blades that rotate a shaft on which the rotor of the synchronous generator with permanent magnets is mounted. The rotor consists of a permanent magnet, which generates a rotating magnetic field obtained mechanically, leading to the generation of electromotive forces at the level of the three-phase windings of the stator [87].

4.1.2. Simulation of the wind mathematical model

Using Simulink software, a block diagram of a horizontal-axis wind turbine will be implemented to analyze the modeling of the characteristics and phenomena that arise. This involves defining the mathematical relationships that describe the interaction of the turbine with the wind, the generator, and other system components. Additionally, turbine parameters, such as the performance coefficient, the blade pitch angle, etc., must be established to accurately reflect a real-world environment.

To obtain concrete values in the simulation, it was necessary to estimate the mechanical losses of the wind turbine due to incomplete specifications, considering losses of 1-3% of the total power for high-quality bearings and 1-2% for internal aerodynamic friction. Thus, the overall mechanical efficiency of the transmission system was set at 97%, the generator efficiency at 95%, and the wind controller efficiency was considered to be 97%. These constants will be

integrated into the Simulink block diagram to determine the useful electrical power generated by the wind turbine according to formula (4.1.).

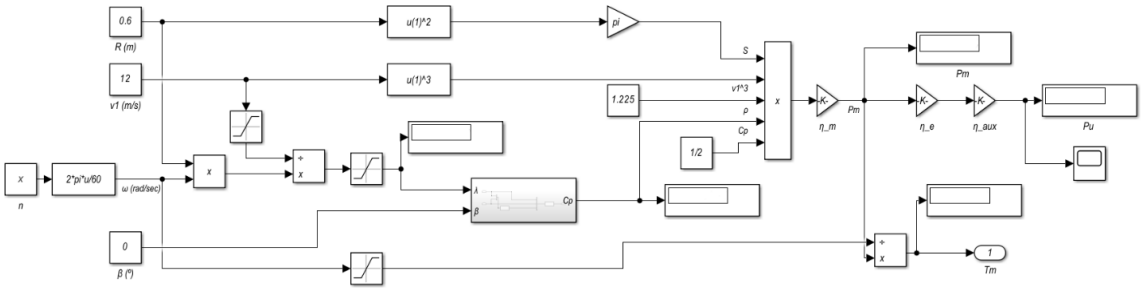

Fig. 0.1. Schema bloc pentru determinarea puterii electrice utile generate de turbina eoliană

In the block diagram shown in figure 4.1., formula (4.9) has been integrated to determine the angular speed of the rotor as a function of the rotational speed, since measurements at different wind speeds will be carried out in the experimental section using a tachometer. The rotational speed of the wind turbine generator's rotor will be used as an input data for the simulation.

4.1.3. Simulated results

To ensure the highest possible accuracy of the simulated data, input values were taken from the experimental section, where the wind speed was measured with an anemometer and the rotor's rotational speed was determined using a tachometer. This approach will allow for a direct validation of the simulated data by comparing it with the actual measured values, ensuring a close correlation between the experimental results and those obtained from the simulations.

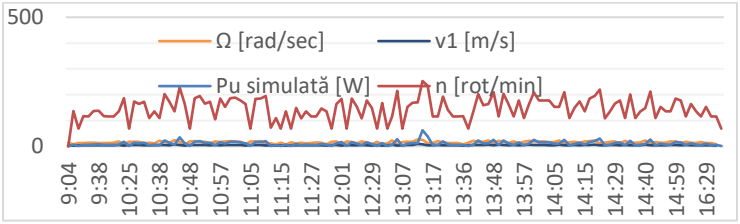

Fig. 0.2. Variation over time of the measured and simulated data

Analyzing the graph of values obtained from the simulations, a direct proportional relationship can be observed between the useful electrical power generated by the wind turbine and the wind speed. This results from the fact that, as the wind speed increases, the airflow available to the turbine rotor is greater, which leads to a significant increase in the power captured and converted into useful electrical energy.

The method of integrating experimental data as input values in the simulation process allowed for a rigorous calibration of the mathematical model. The simulation generated detailed information about the performance coefficient, such as the useful electrical power generated by the wind turbine, and these results will later be compared with the experimental data obtained during tests conducted in real field conditions.

4.2. PHOTOVOLTAIC PANELS

4.2.1. Mathematical models for the photovoltaic energy conversion system

A photovoltaic cell can be considered as a current generator and can be represented by the equivalent circuit shown in Fig 4.3.

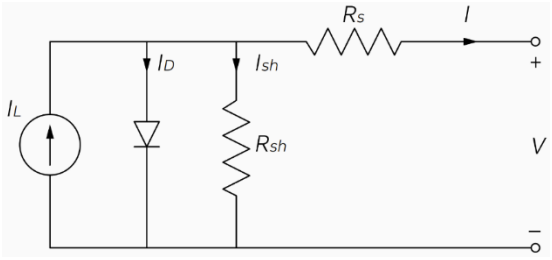

Fig. 0.3. Equivalent circuit configuration of a photovoltaic cell with a single diode [88]

The basic equation for the equivalent circuit configuration of a photovoltaic cell with a single diode (Fig. 4.3.) is defined using Kirchhoff's current law for the current I [88], [89], [90], [91], [92]:

$$I = I_L - I_D - I_{sh} \tag{4.14}$$

where:
I, is the generated current;
I_L, is the light-generated current in the cell;
I_D, is the current lost through the diode, dependent on the voltage;
I_{sh}, is the current lost due to the shunt resistance [88], [89], [90], [91].

The light-generated current in the cell is defined as:

$$I_L = \left(I_{sc\_T} + K_i(T_c - T_{ref})\right) \cdot S \tag{4.15}$$

where:
I_{sc}, is the short-circuit current as a function of temperature;
K_i, is the temperature coefficient of the short-circuit current;
T_c, is the temperature of a cell in Kelvin (K);
T_{ref}, is the reference temperature in Kelvin (K);
S, is the solar radiation in kW/m^2 [89], [90], [91].

To measure solar radiation in W/m², we can rewrite formula (4.15) as:

$$I_L = \left[I_{sc} + K_i(T_c - T_{ref})\right] \cdot \frac{S}{1000} \tag{4.16}$$

Another formula used to determine the light-generated current in the cell is:

$$I_L = \left[I_{sc} + K_i(T_c - T_{ref})\right] \cdot \frac{S + S \cdot Alb(1 - \cos\Theta)}{1000} \tag{4.17}$$

where:
Alb, is the albedo factor;
Θ, is the angle of incidence of the solar radiation.

The short-circuit current can be defined as a function of temperature as follows:

$$I_{sc\_T} = I_{sc}\left[1 + K_i(T_c - T_{ref})\right] \tag{4.18}$$

In the equivalent circuit of the single-diode model, I_D is modeled using the Shockley equation for an ideal diode as follows [88], [89], [90], [91], [92]:

$$I_D = I_0 \cdot \left(e^{\frac{V + IR_s}{nV_T}} - 1\right) \tag{4.19}$$

where:

n, is the ideality factor of the diode, a unitless parameter, which for a single-junction cell typically ranges from 1 to 2;
V, is the cell voltage;
R_s, is the series resistance.

I_0, is the saturation current given by the formula [89], [91]:

$$I_0 = \left(\frac{I_{RS}T_c}{T_{ref}}\right)^3 \cdot e^{\frac{qE_g\left(\frac{1}{T_{ref}} - \frac{1}{T_c}\right)}{kn}} \tag{4.20}$$

where:
E_g, is the bandgap energy of the semiconductor material used in the solar cells.

I_{RS}, is the reverse saturation current given by the formula [91]:

$$I_{RS} = \frac{I_{sc\_T}}{e^{\frac{qV_{oc}}{nkT_c}} - 1} \tag{4.21}$$

where:
V_{oc}, is the open-circuit voltage.

The open-circuit voltage can be defined as a function of temperature as follows:

$$V_{oc\_T} = V_{oc}\left[1 + K_v(T_c - T_{ref})\right] \tag{4.22}$$

where:
K_v, is the temperature coefficient of the open-circuit voltage;

V_T is the thermal voltage given by the formula [88], [89], [90], [91], [92]:

$$V_T = \frac{kT_c}{q} \tag{4.23}$$

where:
k, is Boltzmann's constant (1.381×10^{-23} J/K);
q, is the charge of the electron (1.6×10^{-19} C) [88], [89].

I_{sh}, is the current lost due to the shunt resistance, given by the formula [88], [89], [90], [91], [92]:

$$I_{sh} = \frac{V + IR_s}{R_{sh}} \tag{4.24}$$

where:
R_{sh}, is the shunt resistance.

Thus, the current supplied to the load is given by the following formula [88], [89], [90], [91], [92]:

$$I = I_L - I_0 \cdot \left(e^{\frac{V+IR_s}{nV_T}} - 1\right) - \frac{V + IR_s}{R_{sh}} \tag{4.25}$$

In typical solar cells, the leakage current I_{sh} is usually very small compared to the other two currents in the equation, thus becoming negligible. Therefore, the saturation current of the diode can be experimentally determined by applying an open-circuit voltage V_{oc} to a cell that is not exposed to light and measuring the current passing through it [88].

4.2.2. Simulation of the photovoltaic mathematical model

This section aims to present the simulation process of the mathematical model of a photovoltaic system in Simulink, highlighting its importance in evaluating the performance of real systems. By simulating various operating scenarios and adjusting input parameters, valuable insights can be obtained about the photovoltaic system's behavior under different conditions, thus contributing to improving its efficiency and reliability.

The mathematical model of the photovoltaic panel was developed based on the fundamental equations that describe the electrical behavior of solar cells.

In the final stage of the simulation, the block diagram for calculating the current generated by the photovoltaic panel was developed, taking into account all relevant parameters according to formula (4.25):

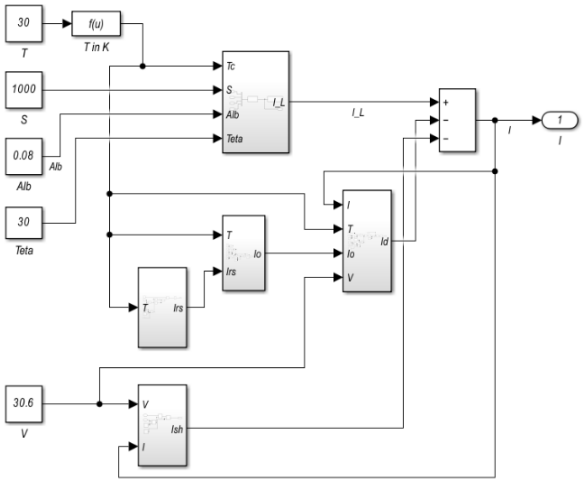

Fig. 0.4. Block diagram for calculating the current generated by the photovoltaic panel, I

This block diagram provides a clear and structured representation of how the variables and parameters interact to determine the current produced, considering the effects of various operating conditions and characteristics of the photovoltaic system.

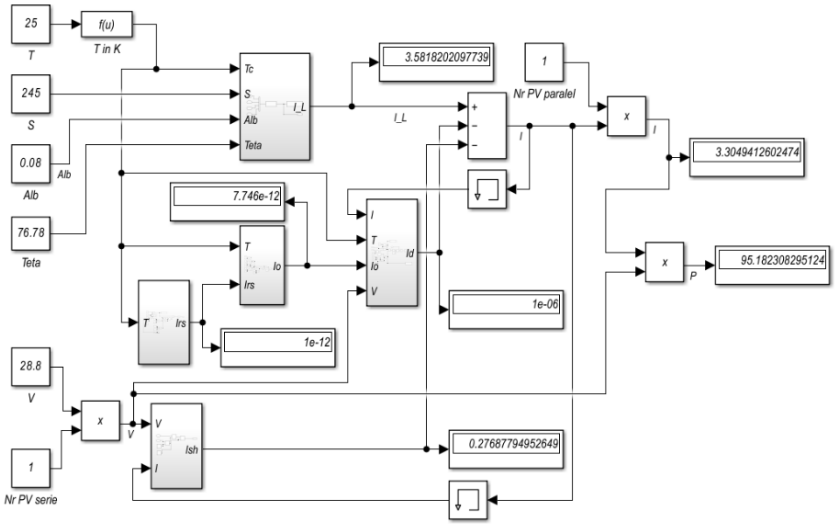

Fig. 0.5. Block diagram for determining the electrical power generated by the photovoltaic panel

4.2.3. Simulated results

To obtain relevant and accurate simulated data, a series of experimental parameters were used as input data for the mathematical model of the photovoltaic panel in Simulink. These experimental data include the voltage generated by the panel, measured solar radiation, and the temperature at the photovoltaic cell level. Additionally, the angle of incidence of solar rays on the panel was calculated precisely, taking into account the day, hour, and minute when the measurements were taken. This incidence angle was determined through the analysis and integration of the four main angles that contribute to its formation, thus ensuring the accuracy of the simulated data. Using this approach, we were able to obtain the current and power generated by the panel, which were then used as simulated data for model validation.

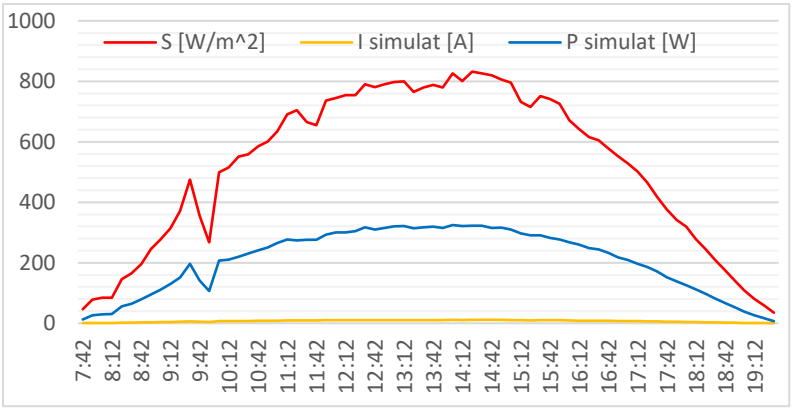

Fig. 0.6. Simulated power and current as a function of solar radiation over time

The method of using experimental data as input for the simulation provided the advantage of offering precise calibration of the mathematical model. The simulation yielded a series of data regarding the power generated and the current produced by the photovoltaic panel. These results will be compared with the experimental data collected during field tests.

4.3. INTEGRATED SIMULATION OF THE HYBRID SYSTEM

This subsection presents the integrated simulation of the hybrid renewable energy system, composed of the renewable energy sources: wind and photovoltaic. Simulations for each subsystem were performed in Simulink, using mathematical models specific to each technology.

The wind turbine simulation was based on key parameters such as rotor radius and blade pitch angle, considered constant, while the input variables included wind speed and rotor speed. For the photovoltaic system, the albedo was treated as a constant value, and the input variables included solar radiation, temperature, voltage taken from the experimental part, and the calculated angle of incidence of solar rays on the panel.

The wind system simulation included all efficiencies and power losses, from mechanical losses in the transmission part to the efficiency of the synchronous generator and the wind controller. Subsequently, in the experiment, data on the output power generated by the turbine after the wind controller will be obtained, where an intelligent resistor was integrated for parameter measurement. These experimental values will be compared with the data obtained from the simulation.

In the simulation of the photovoltaic system, relating to the experimental configuration, measurements will be collected via the solar charge controller, which has input ports for the photovoltaic panel and output ports for the battery storage, thus acquiring data for both types of connections. The mathematical model analyzed the parameters obtained from the photovoltaic panel, but for a realistic evaluation in the final stage of the hybrid system, relevant data refer to the charging of the battery storage. Therefore, it is necessary to integrate the efficiency of the solar charge controller into the block diagram of the photovoltaic system simulation.

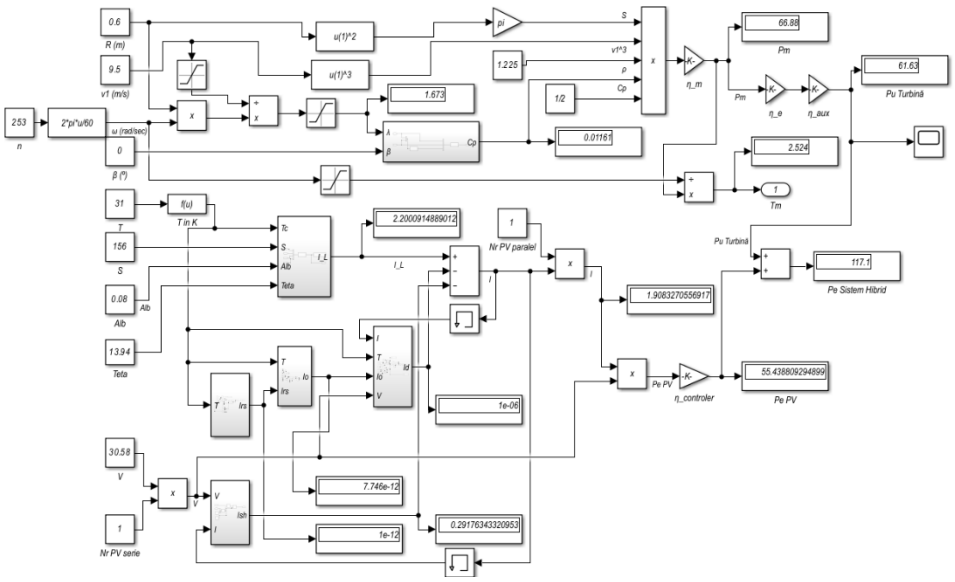

Fig. 0.7. Block diagram of the hybrid system in Simulink

The simulation conditions included variations in the previously mentioned experimental parameters as input data, and the equipment efficiencies were simplified, being included in the calculations to evaluate the overall performance of the hybrid system.

The integration of the simulations was achieved by accumulating the power generated by each system separately, according to the theoretical principle of connecting renewable sources in parallel, where the electrical powers add up [93], [94]. The input parameters of the simulation were taken from real-time experimental measurements.

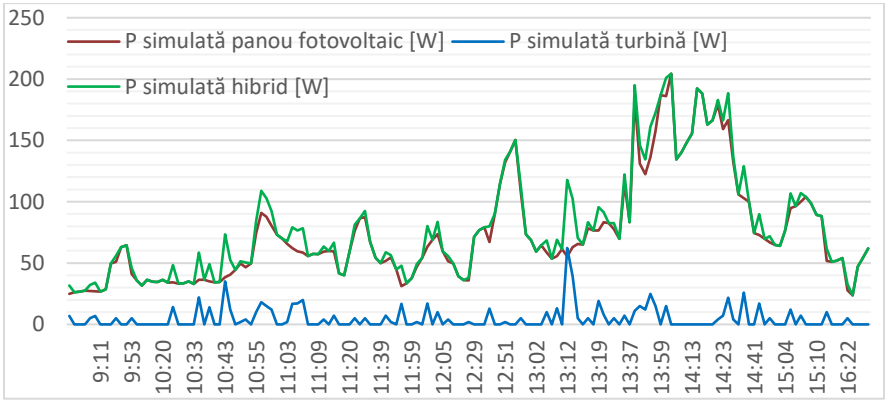

Fig. 0.8. Time variation of the simulated powers in Simulink

After performing the simulation values for the wind-photovoltaic hybrid system, the obtained results provide an initial evaluation of the theoretical behavior of the system under various operational scenarios. These simulated values allow us to analyze the energy potential and the overall efficiency of the system. At this stage, the system has not yet been validated, so the data require a comparison with the experimental values (field measurements) to confirm the accuracy and viability of the theoretical model.

CHAPTER 5 – EXPERIMENTAL IMPLEMENTATION AND CONTRIBUTIONS TO THE OPTIMIZATION OF HYBRID SYSTEM PERFORMANCE

In this chapter, we will present the experimental achievements and contributions made in the development of hybrid systems. As part of this effort, the design and implementation of two renewable energy systems were carried out: a wind system and a photovoltaic system. The experimental data obtained for each of these systems will be detailed in the following sections, highlighting the technical specifications, testing methods, and performance achieved.

Initially, we will focus on the design of the wind system, explaining the development stages, component selection, and optimization criteria used to maximize energy efficiency. The experimental data collected during performance tests will be presented, followed by an analysis of the results and conclusions drawn.

Subsequently, we will detail the design of the photovoltaic system, following a similar approach. The technical specifications, testing methodology, and experimental results obtained will be discussed, with an emphasis on factors influencing system performance.

Finally, the two systems will be integrated into a hybrid system. This section will include a description of the integration process, an analysis of the synergies between the two energy sources, and an evaluation of the overall performance of the hybrid system.

5.1. DESIGN OF THE WIND SYSTEM

5.1.1. Experimental implementation of the wind system

Through the "Renewable Energy Sources and Electrical Equipment Maintenance" laboratory at the Naval Academy "Mircea cel Bătrân," I had access to equipment and resources that allowed the development of an optimized wind system for various testing conditions. The design process included careful selection of components, their configuration, and integration into a system capable of generating and efficiently managing the energy produced by the horizontal-axis wind turbine. The project involved the development of a fully autonomous wind system, including essential components such as the controller, batteries, and inverter.

After analyzing and detailing all the components necessary for creating an autonomous wind system, I proceeded to the practical stage of designing and implementing it. In this stage, I created the electrical schematic of the entire system, which included the connections and interactions between the wind generator, charge controller, battery bank, inverter, and the variable load consumer system.

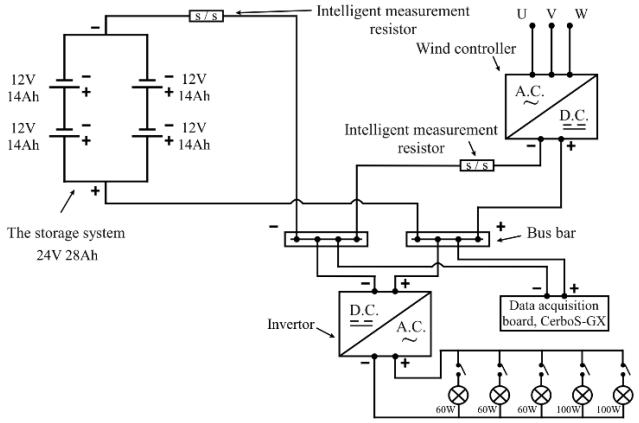

Fig. 0.1. Electrical schematic of the autonomous wind system with variable load

Based on the electrical schematic, the physical implementation of the autonomous wind system was carried out, allowing the collection of relevant experimental data, such as voltage, current, generated power, and system efficiency under various operating conditions, to experimentally evaluate its performance and validate the simulated mathematical model.

5.1.2. Experimental results

Once physically completed, the wind system was installed on the building of the Faculty of Naval Engineering at the "Mircea cel Bătrân" Naval Academy for adjusting the operating parameters of the controller, smart measurement resistors, inverter, and calibrating the data acquisition board for precise monitoring of essential variables, as well as optimizing electrical connections to reduce losses and improve energy efficiency. Experimental data were then collected.

Through the smart measurement resistor connected to the negative terminal at the output of the wind controller, data were monitored and transmitted to the acquisition board, which recorded the following parameters: charging current and voltage, charging power of the battery bank (to be specified in the hybrid system), and useful electrical power generated by the wind turbine. In parallel with this activity, wind speed at the turbine level was measured using a WT816A anemometer. These measurements were crucial to assess the impact of wind conditions on the system's performance.

Fig. 0.2. Measuring wind speed at the level of the horizontal axis wind turbine

The wind turbine rotor speed was measured using a tachometer, enabling the subsequent determination of the rotor's angular speed, which will facilitate the validation of simulated data by comparing it with the values obtained from the experimental side.

The experimental data used in simulations were recorded on 28.08.2024, during a day with moderate wind. Although data were also collected on days with lighter winds, only relevant values corresponding to stronger wind gusts were selected for the final analysis, when the acquisition board collected significant values of the parameters of interest.

These experimental data are essential for verifying and validating the simulated model of the system. By comparing the data obtained during practical tests with the results of the simulations, the accuracy of the theoretical model will be assessed, and any discrepancies will be identified.

The acquisition board received experimental data from the smart measurement resistor, which recorded the following parameters at the output of the wind controller: the useful electrical power of the wind turbine, current, voltage, and the charging power for the battery bank (the last three parameters will be used in validating the hybrid system).

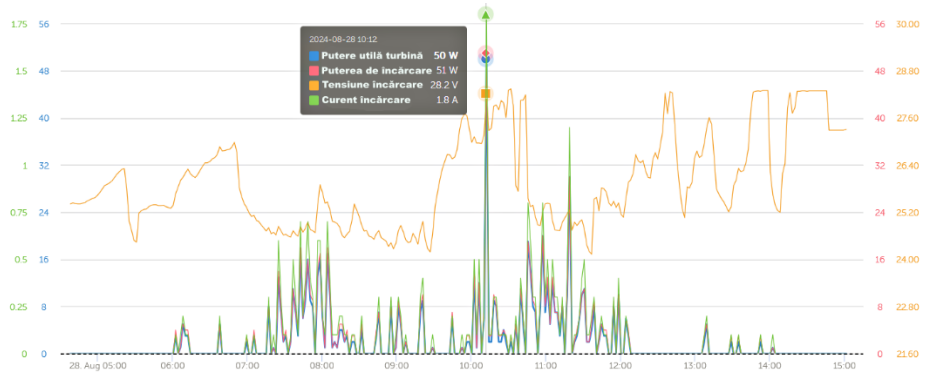

Fig. 0.3. All parameters of the turbine acquired by the smart measurement resistor

5.1.3. Validation of experimental and simulated data

The following subsection details the process of validating experimental and simulated data for the 200W wind turbine. Validation is a crucial step in ensuring the accuracy of the mathematical model in the simulations. By comparing the experimental data obtained under real testing conditions with the results generated by the mathematical model in the simulation, the degree of concordance between the actual behavior of the turbine and the theoretical predictions can be assessed. This analysis will allow for identifying any deviations and appropriately adjusting the model parameters.

By applying the relative error calculation method, we were able to compare the simulated values with those obtained from real experiments, identifying any discrepancies or minor deviations. This approach allowed for a detailed evaluation of the model's accuracy, while also providing essential information about potential improvements needed. With the relative error staying within limits under 1.69%, we can confirm that the developed mathematical model successfully reflects the behavior of the wind system, making it a reliable tool for future analyses and predictions.

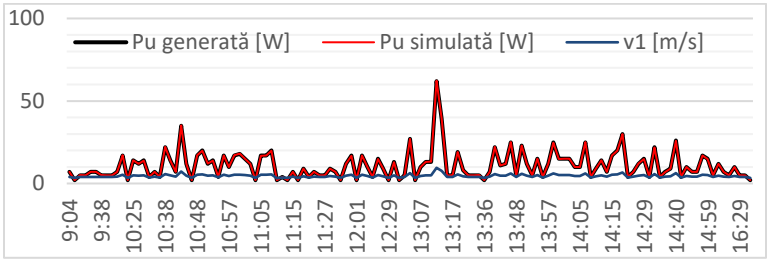

Fig. 0.4. Variation over time of real and simulated values of useful electrical power

5.2. DESIGN OF THE PHOTOVOLTAIC SYSTEM

5.2.1. Experimental implementation of the photovoltaic system

In the subchapter "Design of the Wind System," I detailed all the components necessary for a complete autonomous system. The photovoltaic system will include all the previously specified elements, except for the horizontal-axis wind turbine and its controller. In this section, we will focus exclusively on the specifics of the photovoltaic system, addressing components that were not mentioned in the context of the wind system. We will explore in detail the aspects related to the design and integration of photovoltaic components and collect relevant experimental data to evaluate the performance of this system, thus ensuring a comprehensive and accurate analysis.

After detailing the specific components that will be integrated into the photovoltaic system, I proceeded with the creation of the electrical diagram. This diagram was designed to ensure optimal system operation, taking into account the particularities of the selected equipment.

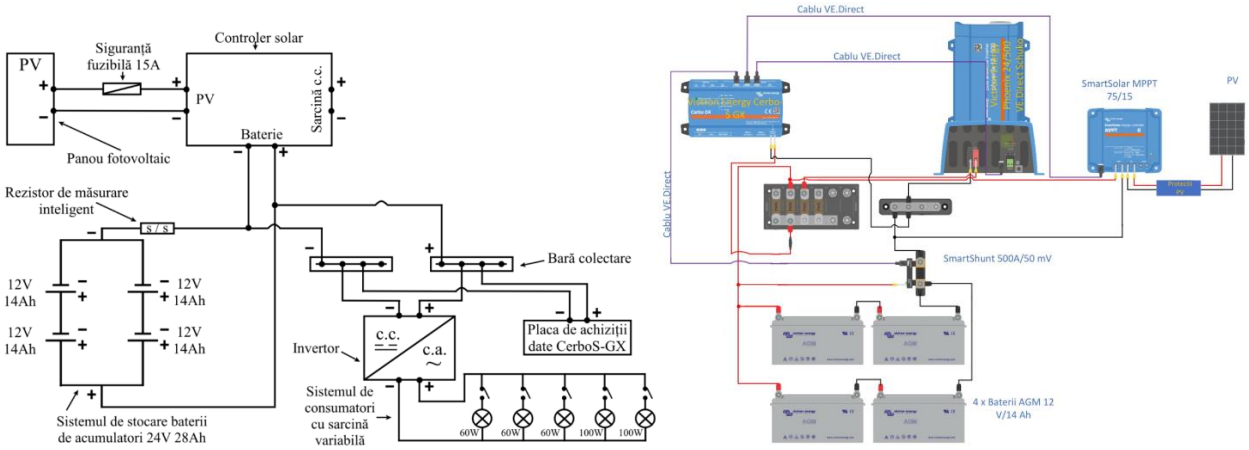

Fig. 0.5. Electrical diagram of the photovoltaic system

5.2.2. Experimental results

After completing the photovoltaic system, we obtained experimental data on the voltage and power generated by the photovoltaic panel using the data acquisition board. In this subchapter, we focus exclusively on analyzing the electricity production. The solar radiation incident on the inclined surface was measured using a PYR1307 pyranometer.

Fig. 0.6. Measuring solar radiation on the inclined surface with the PYR1307 pyranometer

Experimental data were collected on a clear day with 1/8 cloud cover to validate the mathematical model created in the Simulink simulation. To ensure the accuracy and efficiency of the model, measurements were recorded on both sunny and cloudy days, during the period from 02.08.2023 to 13.09.2023. The experimental measurements from 23.08.2023 provide a solid basis for comparing the theoretical and real performance of the constructed photovoltaic system.

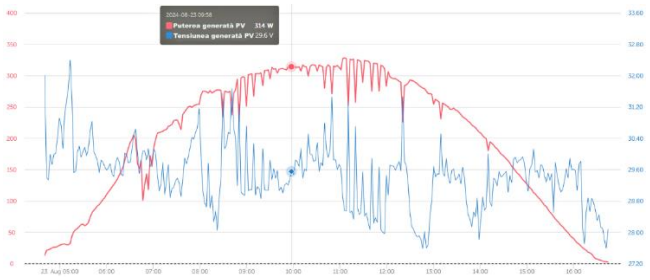

Fig. 0.7. Power and voltage generated by the 395W photovoltaic panel

The data acquisition board received real-time information from the solar charge controller, which recorded important parameters related to the voltage and power generated by the photovoltaic panel (data used to validate the mathematical models for the photovoltaic system), as well as the values of current, voltage, and battery charging power (data used in the validation process for the hybrid system simulations).

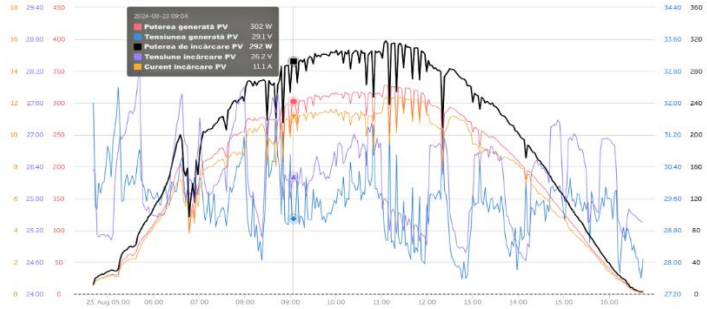

Fig. 0.8. All parameters recorded by the solar charge controller

5.2.3. Validation of experimental and simulated data

An essential component of any research process is the verification and validation of the results obtained through simulation against experimental data. In this case, to ensure the relevance and accuracy of the mathematical model developed for the photovoltaic system, it is crucial to analyze how well the simulated values match those obtained experimentally.

During the experiment, the data acquisition board recorded the voltage and power values generated by the photovoltaic panel at the solar charge controller every minute, allowing us to calculate the current generated by the photovoltaic panel under real conditions.

In the simulation, the basic mathematical model for the equivalent circuit configuration of a photovoltaic cell with a single diode was used, and the input data included: solar radiation, cell temperature, angle of incidence of sunlight on the inclined surface of the panel, and the voltage experimentally measured by the panel. Following the simulation in the Simulink software, the current value and, implicitly, the simulated power of the panel were obtained.

To validate the simulated data against the experimental ones, we used the relative error formula. Based on the error calculation formulas mentioned earlier and utilizing the data obtained both experimentally and through simulation, a table was created presenting the relevant differences between the respective values.

.

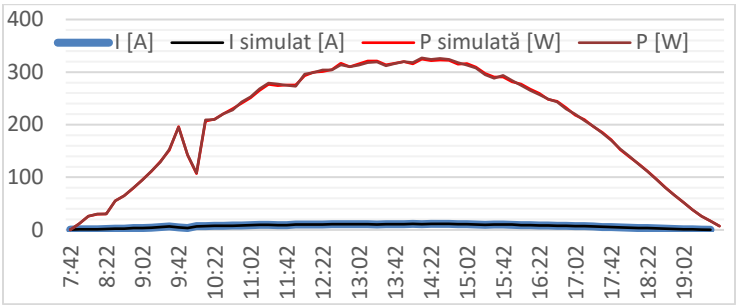

Fig. 0.9. Time variation of experimental current and power compared to simulated values

The simulated data for the photovoltaic system were validated through a rigorous comparison with the measurements obtained experimentally, allowing for an accurate assessment of the mathematical model's accuracy. Following this detailed analysis, it was found that the maximum relative error between the simulated and experimental values was only 1.1%, an outstanding result that demonstrates the model's ability to replicate the real performance of the photovoltaic system with high precision. This relatively small error reflects the fact that key parameters such as solar radiation intensity, conversion efficiency, and operating conditions were well correlated in the simulation, thus providing a solid basis for extrapolating the results and applying them to practical scenarios. Therefore, this validation confirms that the model is suitable for accurate predictions and for the subsequent evaluation of the photovoltaic system's behavior under different operating conditions.

5.3. DESIGN OF THE HYBRID SYSTEM

5.3.1. Creating of the hybrid energy generation system

When two renewable energy sources are connected to a distribution bus, the total generated power will be the sum of the powers provided by each source, provided that they are properly synchronized and compatible in terms of voltage and frequency (for AC) [93], [94], [95], [96].

After the equipment was calibrated according to the specific requirements of our system and issues related to incorrect connections were resolved, the electrical diagram and connection scheme were created. These diagrams ensured a clear and coherent organization of the system components, facilitating the correct implementation of all the necessary electrical connections for the proper functioning of the assembly.

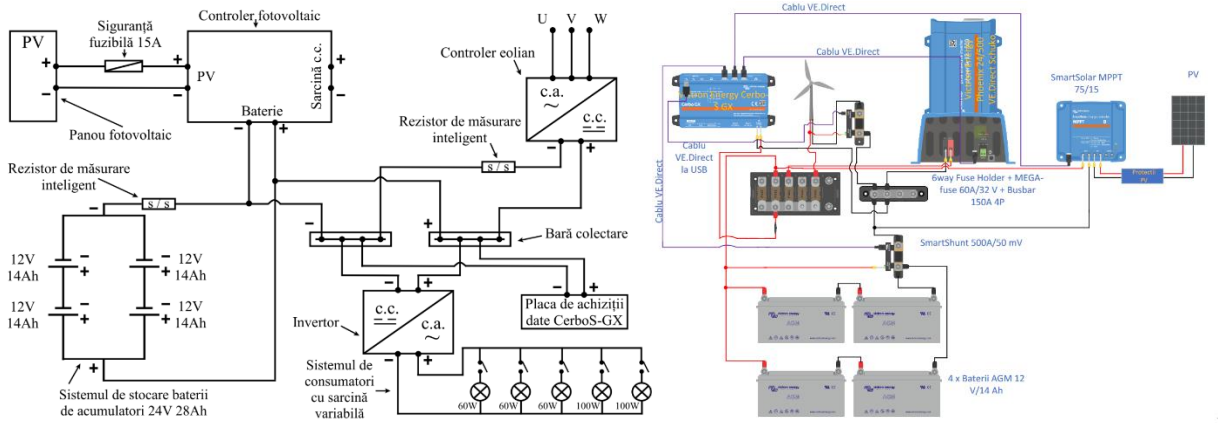

Fig. 0.10. Electrical diagram of the wind-solar hybrid system

In our case, we have a 200W wind turbine generating alternating current (AC), which is converted to direct current (DC) through a wind controller, and a 395W photovoltaic panel connected to the batteries through a solar charge controller. The two sources are connected to the distribution bus, meaning that both supply the battery and the consumer system with DC power. The total available power at the distribution bus is theoretically the sum of the powers generated by both sources, depending on environmental conditions (wind intensity and solar radiation) [93], [94], [95]. If both sources are operating at maximum capacity, the total available power would be 595W.

Fig. 0.11. The 2 renewable energy sources installed on the Faculty of Naval Engineering building

From an energy management and distribution perspective, the wind and solar controllers regulate the flow of energy to the batteries and consumers, eliminating the risk of desynchronization (as would be the case with AC). The energy produced by the renewable sources will charge the batteries and power the consumers depending on the system's requirements and the state of charge of the battery banks. When the energy produced by both sources exceeds consumption, the excess energy will charge the batteries. If consumption exceeds the produced energy, the system will draw power from the batteries. Depending on the resistance of the circuits and the connecting components, small imbalances may occur in the current flow between the sources and the distribution bus; however, these are generally managed by the controllers.

5.3.2. Experimental results from testing the hybrid energy system

This subsection presents the experimental results obtained through the data acquisition board after practical tests were conducted on the hybrid system, consisting of two renewable energy sources: wind and photovoltaic. The measurement steps were previously elaborated and detailed for each component, using a rigorous methodology to obtain the reference values necessary for validating the simulated mathematical model.

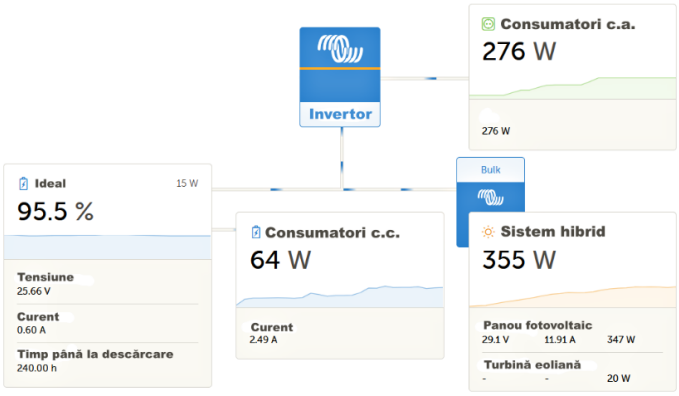

Fig. 0.12. Real-time data acquisition

The day of 28.08.2024 was strategically chosen due to favorable weather conditions for a detailed evaluation. The full cloud cover (8/8) limited the performance of the photovoltaic panel, while still allowing for an in-depth analysis of the wind turbine's energy production. On that day, moderate wind gusts provided favorable moments for recording essential parameters of the turbine, contributing to the collection of precise data for evaluating the hybrid system. These experimental measurements are crucial for correlating the results with theoretical simulations and validating the system's performance under varying weather conditions.

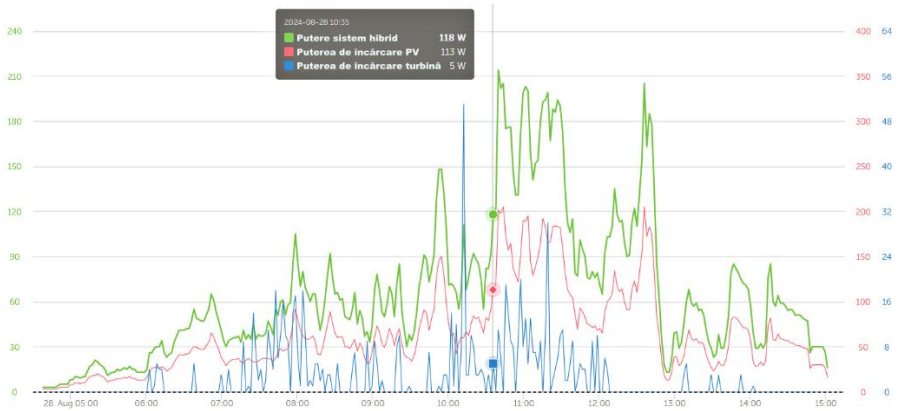

Fig. 0.13. Time variation of hybrid system's charging power

The system produced electrical energy according to environmental conditions, namely wind for the wind turbine and solar radiation for the photovoltaic panel. In addition to energy production, the system also had its own consumption. The internal DC power consumption was generated by the necessary electronic equipment, such as the data acquisition board, smart measuring resistors, and the inverter. Furthermore, there was an external AC power consumption at the inverter's output, which powered the consumer system with variable steps.

The energy produced by the entire system was used to cover both internal and external consumption, with any surplus directed towards charging the batteries. Depending on the energy demand from the consumers and the environmental conditions, the energy stored in the batteries was used to compensate for insufficient production. The battery charging and management algorithm ensured the protection of the batteries against excessive discharge, maintaining a balance between system production and total consumption.

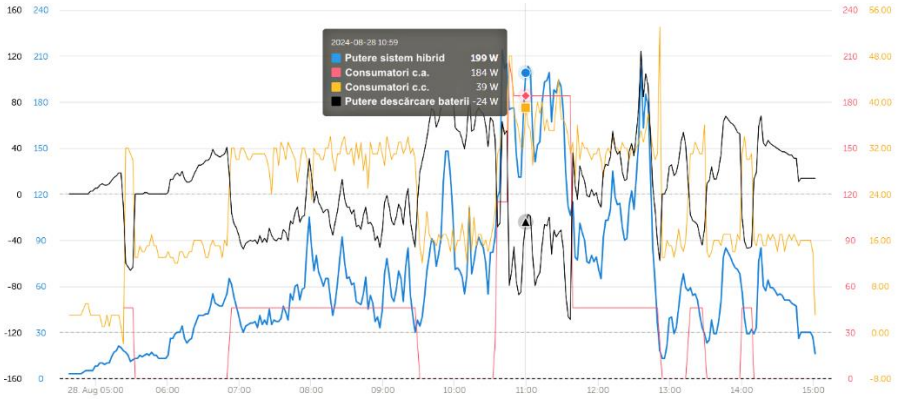

Fig. 0.14. Operation of the hybrid system connected to the consumer system with variable load

5.3.3. Validation of experimental and simulated data

In the simulation of the hybrid renewable energy system, the values obtained for the power generated by each subsystem were combined to analyze overall performance. The simulations indicated that the total power generated by the hybrid system fell within the expected limits based on experimental data. For the wind turbine, the simulations produced a variable average power depending on the wind speed, while for the photovoltaic system, the generated power was correlated with variations in solar radiation and temperature.

On 28.08.2024, under conditions of lower solar radiation and moderate winds, the combined power of the system reached a maximum value of 204 W, while the mathematical model simulated a value of 204.38 W. Analyzing the minimum value recorded by the hybrid system, it generated 26 W, while the simulation in Simulink predicted a value of 26.28 W, confirming an accurate prediction of the generated power. Based on the actual data from the hybrid system, the following values were obtained: for the wind turbine, the generated power varied between 2.42 and 62.59 W, depending on the real wind speed measured, while the simulation determined values between 2.01 and 62.27 W. The photovoltaic system produced power values ranging from 23.21 to 210.17 W, depending on solar radiation, cell temperature, and the angle of incidence of sunlight on the panel, while the mathematical model in Simulink produced values between 24.78 and 204.38 W.

The main objective was to validate the simulated results by comparing them with the real data obtained from testing. During this validation process, it was found that the relative error did not exceed the threshold of 2%, ensuring the accuracy of the mathematical model and its correlation with the practical performance of the hybrid system.

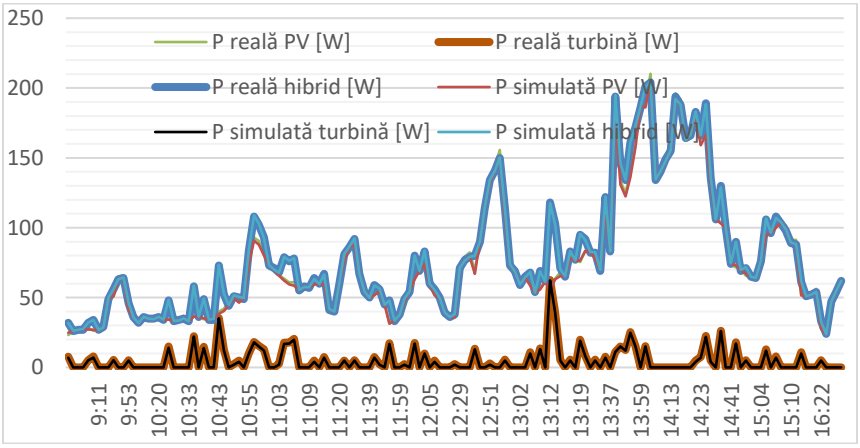

Fig. 0.15. Real and simulated powers of the hybrid wind-photovoltaic system

The simulated model for the wind component is well-calibrated for the range of low experimental values, indicating a good validation. The simulation for the photovoltaic part shows slightly higher errors, particularly in the middle power range (where the sun may be partially covered by clouds), due to the efficiency of the solar charge controller at the output, which does not maintain a constant peak efficiency of 98%. The simulation for the total power is accurate, and the differences between experimental and simulated values are minor, suggesting that the overall model works well for predicting the generated hybrid power. These conclusions support the validation of simulated data with experimental data in the PhD thesis, demonstrating that the model for the wind-photovoltaic hybrid system is efficient.

CHAPTER 6 - CONCLUSIONS AND DEVELOPMENT PERSPECTIVES

6.1. PERSONAL CONTRIBUTIONS

One of the main contributions of the thesis is the **development of an original mathematical model** created specifically to simulate the complex interactions between the components of a wind-photovoltaic hybrid system. This model makes a significant contribution to the field of renewable energy by its ability to simultaneously integrate a variety of dynamic variables and provide accurate predictions of the system's behavior based on fluctuating weather conditions. Unlike traditional models, which often treat each energy source separately and use simplified approximations to assess interactions between them, the model developed in this thesis takes into account the rapid and often unpredictable variations in wind speed and solar radiation intensity. This more complex approach not only allows for more realistic simulations but also facilitates the dynamic adaptation of the model to real operating conditions, offering efficient solutions for managing the variability of energy production.

Another major personal contribution is the **creation of an experimental prototype** that allowed the theoretical validation of the developed mathematical model. Through this prototype, a direct comparison was made between the simulated and real-world measured data, providing a practical confirmation of the model's functionality and accuracy. The development of the prototype required an interdisciplinary approach, involving not only theoretical knowledge from mathematics and physics but also technical skills in circuit design, energy parameter measurement, and optimization of the hybrid system components. This stage of the research clearly demonstrated that the proposed model not only works in simulated conditions but can also be successfully implemented in real physical systems. Real-time measurements taken from the prototype revealed a very good correlation between the theoretical results and the system's field performance, thus confirming the validity of the adopted approach.

The development of an autonomous hybrid system capable of operating in variable and challenging environments represents another important contribution. Thanks to its autonomy, the system reduces dependence on external energy grids, a major advantage for use in isolated environments. An essential aspect of this contribution is the system's ability to automatically adjust its operating parameters based on the availability of renewable resources and consumption needs. This allows it to effectively manage battery charging and discharging, as well as direct energy to the most relevant consumers at any given moment.

Moreover, this research opens new perspectives for the development of similar hybrid systems in other critical fields, such as powering isolated homes or research bases in Arctic regions, where energy fluctuations and extreme conditions demand innovative and efficient technological solutions. By integrating different renewable sources into a single system capable of responding quickly and precisely to resource variations, the contributions of this thesis provide a solid starting point for expanding the use of renewable energy in varied and challenging contexts. Additionally, **the proposed mathematical model can be adapted and extended to incorporate other renewable energy sources**, such as biomass or hydro energy, thus broadening its applicability in different and complex scenarios.

In conclusion, this research makes significant contributions both theoretically and practically, not only by developing and validating an innovative mathematical model but also by creating a functional prototype that can be successfully applied in real-world situations.

REFERENCES

[1] H. Kang, S. Han, C. An, and Y.-K. Kim, "Design Process of a Small-Scaled Bladeless Vortex-Induced Wind Turbine with Tunable Resonance Mechanism," *2024 IEEE 22nd Int. Conf. Ind. Informatics*, pp. 1–6, Aug. 2024, doi: 10.1109/INDIN58382.2024.10774332.

[2] D. Han, S. Huang, P. K. Abia Hui, and Y. Chen, "Development of a New Type of Vortex Bladeless Wind Turbine for Urban Energy Systems," *2024 9th Int. Conf. Power Renew. Energy, ICPRE 2024*, pp. 973–978, 2024, doi: 10.1109/ICPRE62586.2024.10768593.

[3] H. Y. Kang and Y. K. Kim, "Development of Smart-Rubber Based Resonance Tuning Module for Bladeless Wind Turbine System," *Int. Conf. Control. Autom. Syst.*, pp. 1830–1833, 2023, doi: 10.23919/ICCAS59377.2023.10316880.

[4] W. Barday, Z. S. Bahri, S. Ez-Zabri, and Y. Salih-Alj, "An Off-Grid Hybrid Piezoelectric-Electromagnetic Tuning System for Vortex Induced Vibration Bladeless Turbines," *Colloq. Inf. Sci. Technol. Cist*, pp. 342–349, 2023, doi: 10.1109/CIST56084.2023.10409962.

[5] P. K T, T. K. Makanur, P. R, M. M, V. G. S, and K. Manickavasagam, "Design and Analysis of a Miniaturized Vortex Induced Wind Turbine," pp. 1–6, Jul. 2024, doi: 10.1109/AMATHE61652.2024.10582248.

[6] V. Bhardwaj and A. V. Ravi Teja, "Mathematical Modelling and Equivalent Circuit Representation of Bladeless Wind Turbines," *IECON Proc. (Industrial Electron. Conf.*, vol. 2021-October, Oct. 2021, doi: 10.1109/IECON48115.2021.9589902.

[7] A. C. R. Buela *et al.*, "Design and Nonlinear Static Simulation of a Small-Scale Vortex Bladeless Wind Power Generator," *2021 IEEE Int. Conf. Autom. Control Intell. Syst. I2CACIS 2021 - Proc.*, pp. 185–190, Jun. 2021, doi: 10.1109/I2CACIS52118.2021.9495882.

[8] F. E. Tonny, M. K. Hassan kajal, T. Anam, A. M. Tafikul Islam, M. R. Mobarrat, and M. Hassan, "Optimizing Community Energy with Smart Hardware Integration in Offline Microgrid Systems," *2024 IEEE Int. Conf. Power, Electr. Electron. Ind. Appl.*, pp. 1–6, Sep. 2024, doi: 10.1109/PEEIACON63629.2024.10800723.

[9] S. Pol, B. C. Houchens, D. V. Marian, and C. H. Westergaard, "Performance of aeromines for distributed wind energy," *AIAA Scitech 2020 Forum*, vol. 1 PartF, pp. 1–8, 2020, doi: 10.2514/6.2020-1241.

[10] "Home." https://aerominetechnologies.com/ (accessed Sep. 22, 2024).

[11] S. Pol, C. Westergaard, D. Marian, and B. Houchens, "Pilot-scale performance of AeroMINE at low wind speeds.," 2021, doi: 10.2172/1870762.

[12] S. Budea, A. Ciocănea, and F. Opriș, "Natural Ventilation of Buildings by Using Venturi Devices Placed on the Rooftops," *2023 11th Int. Conf. ENERGY Environ. CIEM 2023*, 2023, doi: 10.1109/CIEM58573.2023.10349752.

[13] "A Norwegian company is working on a wall of floating wind turbines." https://www.cnbc.com/2023/05/16/a-norwegian-company-is-working-on-a-wall-of-floating-wind-turbines.html (accessed Sep. 22, 2024).

[14] "floating 'windcatchers' will rise 1,000 feet to power 80,000 homes each." https://www.designboom.com/technology/norway-wind-catching-systems-wcs-floating-windcatcher-turbine-06-09-2021/ (accessed Sep. 22, 2024).

[15] E. MacMahon and W. E. Leithead, "Performance Comparison of Optimised and Non-Optimised Yaw Control for a Multi Rotor System," *2018 IEEE Conf. Control Technol. Appl. CCTA 2018*, pp. 1638–1643, Oct. 2018, doi: 10.1109/CCTA.2018.8511353.

[16] "Wind Catching Systems." https://www.windcatching.com/ (accessed Sep. 22, 2024).

[17] "Wind Catching Systems designs giant floating wind farm with 117 turbines."

https://www.dezeen.com/2021/08/26/wind-catching-systems-floating-offshore-farm/ (accessed Sep. 22, 2024).

[18] H. Kathuria, I. Singh, A. Gupta, G. Puniya, and B. Kumar, "Analysis of Bifacial Photovoltaic Panel Under Different Reflective Surfaces," *Proc. 3rd IEEE Int. Conf. Power Electron. Intell. Control Energy Syst. ICPEICES 2024*, pp. 933–938, 2024, doi: 10.1109/ICPEICES62430.2024.10719302.

[19] S. K. Magableh, C. Wang, and F. Lin, "Utility-Scale Bifacial Solar Photovoltaic System: Optimum Sizing and Techno-Economic Evaluation," *IEEE Power Energy Soc. Gen. Meet.*, 2024, doi: 10.1109/PESGM51994.2024.10688984.

[20] H. L. Tan *et al.*, "Investigation of Bifacial Gain and Albedo of Bifacial Photovoltaic Modules that Operate in a Tropical Site," *2024 8th Int. Conf. Green Energy Appl. ICGEA 2024*, pp. 265–270, 2024, doi: 10.1109/ICGEA60749.2024.10560565.

[21] M. M. Hoque *et al.*, "Performance Analysis of a Grid Integrated Bifacial Solar Energy System for Dhaka-Mawa Expressway," *2023 10th IEEE Int. Conf. Power Syst. ICPS 2023*, 2023, doi: 10.1109/ICPS60393.2023.10428925.

[22] A. Singh and D. Jones, "Snow Shedding properties of Bifacial PV Panels," *Conf. Rec. IEEE Photovolt. Spec. Conf.*, vol. 2022-June, pp. 646–648, 2022, doi: 10.1109/PVSC48317.2022.9938947.

[23] T. M. Mahim, A. H. M. A. Rahim, and M. M. Rahman, "Weather Responsive Multidimensional Photovoltaic Efficiency Model for Simulation of Custom-Built Bifacial Panel," *IEEE J. Photovoltaics*, vol. 14, no. 5, pp. 848–860, Jul. 2024, doi: 10.1109/JPHOTOV.2024.3421252.

[24] A. Anjum, A. H. Tanveer, M. K. Sikder, A. Arefin, M. Islam, and M. M. Rahman, "Bifacial Module Based Multilevel Solar Panel System: A Comparative Study," *2020 IEEE Reg. 10 Symp. TENSYMP 2020*, pp. 324–327, Jun. 2020, doi: 10.1109/TENSYMP50017.2020.9230649.

[25] J. Li, M. Tang, B. An, and X. Guo, "Research on MPPT Strategy of Bifacial Photovoltaic Power Generation System Based on PSO," *2023 7th Int. Conf. Smart Grid Smart Cities, ICSGSC 2023*, pp. 468–473, 2023, doi: 10.1109/ICSGSC59580.2023.10319179.

[26] R. Mahkeswaran, A. K. Ng, C. Toh, and B. Toh, "Maximising Solar Irradiation of Semi-transparent Solar Panels in a Multi-loop Aquaponics System," *5th Technol. Innov. Manag. Eng. Sci. Int. Conf. TIMES-iCON 2024 - Proc.*, 2024, doi: 10.1109/TIMES-ICON61890.2024.10630753.

[27] K. Nath, B. Nath, M. S. Islam, A. N. Chowdhury, and M. A. Matin, "Exploring the Performance of QDIBSC for Spherical QD Structure," *12th IEEE Int. Conf. Renew. Energy Res. Appl. ICRERA 2023*, pp. 445–450, 2023, doi: 10.1109/ICRERA59003.2023.10269410.

[28] A. Kavga, V. Thomopoulos, and T. Petrakis, "The Contribution of Semi-Transparent Photovoltaics for Energy Autonomy in Aloe Vera Greenhouse Cultivation," *2023 31st Mediterr. Conf. Control Autom. MED 2023*, pp. 85–88, 2023, doi: 10.1109/MED59994.2023.10185759.

[29] H. Apostoleris, K. Younes, and M. Chiesa, "A simple, semi-empirical performance modeling approach for partially transparent tracking-integrated concentrator photovoltaics," *Conf. Rec. IEEE Photovolt. Spec. Conf.*, pp. 1373–1376, Jun. 2021, doi: 10.1109/PVSC43889.2021.9518698.

[30] A. Ponmalar, A. Jose Anand, P. Saravanan, S. Deeba, and J. Br, "IoT Enabled Inexhaustible E-vehicle using Transparent Solar Panel," *2022 Int. Conf. Commun. Comput. Internet Things, IC3IoT 2022 - Proc.*, 2022, doi: 10.1109/IC3IOT53935.2022.9767921.

[31] E. Irmak, M. S. Ayaz, S. G. Gok, and A. B. Sahin, "A survey on public awareness towards renewable energy in Turkey," *3rd Int. Conf. Renew. Energy Res. Appl. ICRERA 2014*, pp. 932–937, Jan. 2014, doi: 10.1109/ICRERA.2014.7016523.

[32] M. Beken, B. Hangun, and O. Eyecioglu, "Classification of turkey among european countries by years in terms of energy efficiency, total renewable energy, energy consumption, greenhouse gas emission and energy import dependency by using machine learning," *8th Int. Conf. Renew. Energy Res. Appl. ICRERA 2019*, pp. 951–956, Nov. 2019, doi: 10.1109/ICRERA47325.2019.8996583.

[33] R. T. Jacob and R. Liyanapathirana, "Technical Feasibility in Reaching Renewable Energy Targets; Case Study on Australia," *Proc. 4th Int. Conf. Electr. Energy Syst. ICEES 2018*, pp. 630–634, Aug. 2018, doi: 10.1109/ICEES.2018.8443251.

[34] S. R. Bull, "Renewable energy today and tomorrow," *Proc. IEEE*, vol. 89, no. 8, pp. 1216–1226, 2001, doi: 10.1109/5.940290.

[35] D. Braga, "Optimal Capacity and Feasibility of Energy Storage Systems for Power Plants Using Variable Renewable Energy Sources," *SIELMEN 2021 - Proc. 11th Int. Conf. Electromechanical Energy Syst.*, pp. 87–91, 2021, doi: 10.1109/SIELMEN53755.2021.9600392.

[36] Z. Tang, Y. Yang, and F. Blaabjerg, "Power electronics: The enabling technology for renewable energy integration," *CSEE J. Power Energy Syst.*, vol. 8, no. 1, pp. 39–52, 2022, doi: 10.17775/CSEEJPES.2021.02850.

[37] I. Renewable and E. Agency, *Renewable capacity statistics 2016 Statistiques de capacité renouvelable 2016 Estadísticas de capacidad renovable 2016*. 2016.

[38] F. Blaabjerg and K. Ma, "Future on power electronics for wind turbine systems," *IEEE J. Emerg. Sel. Top. Power Electron.*, vol. 1, no. 3, pp. 139–152, Sep. 2013, doi: 10.1109/JESTPE.2013.2275978.

[39] J. Taghinezhad, E. Mahmoodi, M. Masdari, and R. Alimardani, "Spectral Analyses of an Optimized Ducted Wind Turbine using Hot-Wire Anemometry," *7th Iran Wind Energy Conf. IWEC 2021*, May 2021, doi: 10.1109/IWEC52400.2021.9467033.

[40] O. Cristea, M. O. Popescu, F. Deliu, and A. S. Calinciuc, "Dynamic performances of a wind power system," *2014 Int. Symp. Fundam. Electr. Eng. ISFEE 2014*, Feb. 2015, doi: 10.1109/ISFEE.2014.7050635.

[41] Y. Yin, M. Liao, and P. Lyu, "The dynamic stability analysis of wind turbines under different control strategies," *Proc. 5th IEEE Int. Conf. Electr. Util. Deregulation, Restruct. Power Technol. DRPT 2015*, pp. 2581–2586, Mar. 2016, doi: 10.1109/DRPT.2015.7432683.

[42] C. Niţu, A. S. Dobrescu, and A. Oprea, "Sisteme inteligente în ecologie : surse regenerabile de energie : aplicaţii," 2016, Accessed: Aug. 03, 2024. [Online]. Available: https://www.matrixrom.ro/produs/sisteme-inteligente-in-ecologie-surse-regenerabile-de-energie-aplicatii/.

[43] K. Naoi and M. Shiono, "Relationship between Incident Angle of Wind on Rotor Blade and Output of a Drag-type Multi-blade Vertical-Axis Wind Turbine with Stationary Multi-vanes," *2021 11th Int. Conf. Power, Energy Electr. Eng. CPEEE 2021*, pp. 147–152, Feb. 2021, doi: 10.1109/CPEEE51686.2021.9383349.

[44] C. Popa, "Review of renewable energy sources and offshore wind turbine technology.," *Sci. Bull. "Mircea cel Batran" Nav. Acad.*, vol. 24, no. 2, pp. 1–16, 2021, Accessed: Jan. 23, 2025. [Online]. Available: https://openurl.ebsco.com/contentitem/edb:156420514?sid=ebsco:plink:crawler&id=ebsco:edb:156420514&crl=c.

[45] T. Catalina, "Utilizarea surselor de energie regenerabilă în clădiri," 2015, Accessed: Sep.

18, 2024. [Online]. Available: https://www.matrixrom.ro/produs/utilizarea-surselor-de-energie-regenerabila-in-cladiri/.

[46] N. S. Patil and Y. N. Bhosle, "A review on wind turbine generator topologies," *Proc. 2013 Int. Conf. Power, Energy Control. ICPEC 2013*, pp. 625–629, 2013, doi: 10.1109/ICPEC.2013.6527733.

[47] A. Badea and E. Agir, "Adrian BADEA Horia NECULA coordonatori Editura Agir."

[48] M. Bălăceanu, N.-S. Popa, V. Nae, M.-C. Târhoacă, and C. Popa, "State of the Art in Wind Turbine and Photovoltaic Panels," *Tech. Electro*, vol. 2, pp. 1–9, Mar. 2024, Accessed: Jan. 23, 2025. [Online]. Available: https://www.techniumscience.com/index.php/electro/article/view/10751.

[49] M. Liao, L. Dong, L. Jin, and S. Wang, "Study on rotational speed feedback torque control for wind turbine generator system," *2009 Int. Conf. Energy Environ. Technol. ICEET 2009*, vol. 1, pp. 853–856, 2009, doi: 10.1109/ICEET.2009.211.

[50] J. Alshehri, A. Alzahrani, and M. Khalid, "Wind Energy Conversion Systems and Artificial Neural Networks: Role and Applications," *2019 IEEE PES Innov. Smart Grid Technol. Asia, ISGT 2019*, pp. 1777–1782, May 2019, doi: 10.1109/ISGT-ASIA.2019.8881404.

[51] P. Tinglong, J. Zhicheng, and J. Zhenhua, "Maximum power point tracking of wind energy conversion systems based on sliding mode extremum seeking control," *2008 IEEE Energy 2030 Conf. ENERGY 2008*, 2008, doi: 10.1109/ENERGY.2008.4781032.

[52] F. Blaabjerg and K. Ma, "Wind Energy Systems," *Proc. IEEE*, vol. 105, no. 11, pp. 2116–2131, Nov. 2017, doi: 10.1109/JPROC.2017.2695485.

[53] ABB, "Technical Application Papers No.13 Wind power plants," no. 13, p. 136, 2011, [Online]. Available: https://library.e.abb.com/public/92faf0c1913f5651c1257937002f88e8/1SDC007112G0201.pdf.

[54] N. S. Popa, M. G. Manea, C. Popa, V. Mocanu, H. Isac, and M. O. Popescu, "Solar Energy Utilization for Powering Surface Drones: Study on Mathematical Models for Electricity Production Prediction," *UPB Sci. Bull. Ser. C Electr. Eng. Comput. Sci.*, vol. 86, no. 4, pp. 303–314, 2024.

[55] B. Liu, S. Duan, F. Liu, and P. Xu, "Analysis and improvement of maximum power point tracking algorithm based on incremental conductance method for photovoltaic array," *Proc. Int. Conf. Power Electron. Drive Syst.*, pp. 637–641, 2007, doi: 10.1109/PEDS.2007.4487768.

[56] C. Popa, M.-O. Popescu, M. Târhoacă, and N.-S. Popa, "Photovoltaic panels efficiency on the ships," *Tech. Rom. J. Appl. Sci. Technol.*, vol. 14, pp. 45–50, Oct. 2023, doi: 10.47577/TECHNIUM.V14I.9673.

[57] N. S. Popa, O. Cristea, C. Popa, V. Mocanu, and A. I. Dinu, "The Study on the Implementation of High-Power Photovoltaic Systems on Military Platforms," *2023 Int. Symp. Fundam. Electr. Eng. ISFEE 2023*, 2023, doi: 10.1109/ISFEE60884.2023.10637075.

[58] "Photovoltaic Industrial Systems: An Environmental Approach (Green Energy and Technology): Papadopoulou, Elena: 9783642163005: Amazon.com: Books." https://www.amazon.com/Photovoltaic-Industrial-Systems-Environmental-Technology/dp/3642163009 (accessed Sep. 20, 2024).

[59] H. Abbes, K. Loukil, H. Abid, M. Abid, and A. Toumi, "Implementation of a Maximum Power Point Tracking fuzzy controller on FPGA circuit for a photovoltaic system," *Int. Conf. Intell. Syst. Des. Appl. ISDA*, vol. 2016-June, pp. 386–391, Jun. 2016, doi: 10.1109/ISDA.2015.7489260.

[60] K. Amara *et al.*, "Improved Performance of a PV Solar Panel with Adaptive Neuro Fuzzy Inference System ANFIS based MPPT," *7th Int. IEEE Conf. Renew. Energy Res. Appl. ICRERA 2018*, pp. 1098–1101, Dec. 2018, doi: 10.1109/ICRERA.2018.8566818.

[61] B. T. Attayah, A. I. Alzaidi, N. Fasel, and M. Rava, "Enhancing the Photovoltaic System Output Performance through the Use of Maximum Power Point Tracking and Fuzzy Logic Control," *ICPEA 2021 - 2021 IEEE Int. Conf. Power Eng. Appl.*, pp. 68–72, Mar. 2021, doi: 10.1109/ICPEA51500.2021.9417752.

[62] N. Yan, S. Li, T. Yan, and S. H. Ma, "Study on the whole life cycle energy management method of energy storage system with risk correction control," *2020 IEEE 4th Conf. Energy Internet Energy Syst. Integr. Connect. Grids Towar. a Low-Carbon High-Efficiency Energy Syst. EI2 2020*, pp. 2450–2454, Oct. 2020, doi: 10.1109/EI250167.2020.9346933.

[63] G. E. Asimakopoulou, A. L. Dimeas, and N. D. Hatziargyriou, "Leader-follower strategies for energy management of multi-microgrids," *IEEE Trans. Smart Grid*, vol. 4, no. 4, pp. 1909–1916, Dec. 2013, doi: 10.1109/TSG.2013.2256941.

[64] T. Hennessy and M. Kuntz, "The multiple benefits of integrating electricity storage with wind energy," *2005 IEEE Power Eng. Soc. Gen. Meet.*, vol. 2, pp. 1952–1953, 2005, doi: 10.1109/PES.2005.1489366.

[65] C. POPA, I. CHIABURU, and H. ISAC, "REVIEW OF BATTERY TYPES AND APPLICATION TO WIND POWER GENERATION SYSTEM.," *J. Mar. Technol. Environ.*, vol. 2, no. 2, pp. 72–79, Oct. 2023, doi: 10.53464/JMTE.02.2023.12.

[66] N.-S. POPA, C. POPA, V. MOCANU, and L.-M. POPA, "STATE OF THE ART IN BATTERY TECHNOLOGY: INNOVATIONS AND ADVANCEMENTS," *J. Mar. Technol. Environ.*, vol. 2, no. 2, p. 80, Jul. 2023, doi: 10.53464/JMTE.02.2023.13.

[67] S. Teleke, M. E. Baran, S. Bhattacharya, and A. Q. Huang, "Optimal control of battery energy storage for wind farm dispatching," *IEEE Trans. Energy Convers.*, vol. 25, no. 3, pp. 787–794, Sep. 2010, doi: 10.1109/TEC.2010.2041550.

[68] X. Y. Wang, D. M. Vilathgamuwa, and S. S. Choi, "Determination of battery storage capacity in energy buffer for wind farm," *IEEE Trans. Energy Convers.*, vol. 23, no. 3, pp. 868–878, 2008, doi: 10.1109/TEC.2008.921556.

[69] C. Luo and B. T. Ooi, "Frequency deviation of thermal power plants due to wind farms," *IEEE Trans. Energy Convers.*, vol. 21, no. 3, pp. 708–716, Sep. 2006, doi: 10.1109/TEC.2006.874210.

[70] X. Shi *et al.*, "Research on Energy Storage Configuration Method Based on Wind and Solar Volatility," *2020 10th Int. Conf. Power Energy Syst. ICPES 2020*, pp. 464–468, Dec. 2020, doi: 10.1109/ICPES51309.2020.9349645.

[71] C. Xing, X. Xi, X. He, and M. Liu, "Research on the MPPT Control Simulation of Wind and Photovoltaic Complementary Power Generation System," *iSPEC 2020 - Proc. IEEE Sustain. Power Energy Conf. Energy Transit. Energy Internet*, pp. 1058–1063, Nov. 2020, doi: 10.1109/ISPEC50848.2020.9350965.

[72] P. Molotov, A. Vaskov, and M. Tyagunov, "Modeling Processes in Microgrids with Renewable Energy Sources," *Proc. - 2018 Int. Ural Conf. Green Energy, Ural. 2018*, pp. 203–208, Nov. 2018, doi: 10.1109/URALCON.2018.8544313.

[73] A. Wasonga, M. Saulo, and V. Odhiambo, "Solar-Wind Hybrid Energy System for New Engineering Complex- Technical University of Mombasa," *Http://Www.Sciencepublishinggroup.Com*, vol. 4, no. 2, p. 80, 2014, doi: 10.11648/j.ijepe.s.2015040201.17.

[74] G. Wang, J. Zhang, W. Zhang, H. Liu, and X. Cui, "Research on Transient Stability Analysis of Win d-Photovoltaic-Thermal-bundled Power Transmitt ed System," *5th IEEE*

Conf. Energy Internet Energy Syst. Integr. Energy Internet Carbon Neutrality, EI2 2021, pp. 366–370, 2021, doi: 10.1109/EI252483.2021.9713651.

[75] V. Chaudhary, A. Bhargava, and S. Bhasin, "Modeling and Simulation of gird connected hybrid power system integrated with solar PV/Wind and controlled by Voltage Regulator," *Proc. 4th Int. Conf. Commun. Electron. Syst. ICCES 2019*, pp. 1316–1320, Jul. 2019, doi: 10.1109/ICCES45898.2019.9002036.

[76] H. K. V Lotsch *et al.*, *Optical Sciences*. 2007.

[77] Z. R. Labidi and A. Mami, "Study and simulation of a hybrid photovoltaic-wind generator connected to a DC load," *16th Int. Conf. Sci. Tech. Autom. Control Comput. Eng. STA 2015*, pp. 731–736, Jul. 2016, doi: 10.1109/STA.2015.7505101.

[78] C. Popa, N.-S. Popa, H. Isac, A.-D. Deliu, and C. Andronic, "Comprehensive analysis of offshore wind-photovoltaic hybrid systems: unveiling state-of-the-art autonomous components for maritime applications," *Tech. Rom. J. Appl. Sci. Technol.*, vol. 19, pp. 50–58, Feb. 2024, doi: 10.47577/TECHNIUM.V19I.10624.

[79] M. A. S. Masoum, S. M. Mousavi Badejani, and M. Kalantar, "Optimal placement of hybrid PV-wind systems using genetic algorithm," *Innov. Smart Grid Technol. Conf. ISGT 2010*, 2010, doi: 10.1109/ISGT.2010.5434746.

[80] M. Y. Allani, M. Jomaa, D. Mezghani, and A. Mami, "Modelling and simulation of the hybrid system PV-wind with MATLAB/SIMULINK," *2018 9th Int. Renew. Energy Congr. IREC 2018*, pp. 1–6, May 2018, doi: 10.1109/IREC.2018.8362514.

[81] S. T. Broujeni, S. H. Fathi, and J. S. Moghani, "Hybrid PV/wind power system control for maximum power extraction and output voltage regulation," *3rd Int. Conf. Control. Instrumentation, Autom. ICCIA 2013*, pp. 59–64, Sep. 2014, doi: 10.1109/ICCIAUTOM.2013.6912809.

[82] M. Jomaa, M. Y. Allani, F. Tadeo, and A. Mami, "Design and control of the hybrid system PV-Wind connected to the DC load," *2018 9th Int. Renew. Energy Congr. IREC 2018*, pp. 1–6, May 2018, doi: 10.1109/IREC.2018.8362515.

[83] S. Bhamu, N. Pathak, and T. S. Bhatti, "Power control of wind-biogas-PV based hybrid system," *2018 Int. Conf. Comput. Power Commun. Technol. GUCON 2018*, pp. 421–426, Mar. 2019, doi: 10.1109/GUCON.2018.8675057.

[84] T. Catalina, "Utilizarea surselor de energie regenerabilă în clădiri," 2015, Accessed: Nov. 21, 2023. [Online]. Available: https://www.matrixrom.ro/produs/utilizarea-surselor-de-energie-regenerabila-in-cladiri/.

[85] R. Sarkar, S. Julai, C. W. Tong, O. Z. Chao, and M. Rahman, "Mathematical modelling and simulation of induction generator based wind turbine in MATLAB / SIMULINK MATHEMATICAL MODELLING AND SIMULATION OF INDUCTION GENERATOR BASED WIND TURBINE IN MATLAB / SIMULINK," no. April 2016, 2015.

[86] M. Yin, S. Member, G. Li, and M. Zhou, "Modeling of the Wind Turbine with a Permanent Magnet Synchronous Generator for Integration," pp. 1–6, 2007.

[87] M. Jus, "MATHEMATICAL MODEL OF WIND TURBINE IN GRID-OFF SYSTEM," vol. 14, no. 1, pp. 10–13, 2020.

[88] "Photovoltaic plants Cutting edge technology. From sun to socket."

[89] A. Rawan, N. M. Yasin, and A. N. K. Alshamaa, "Design and Simulation of a Grid Tied Single Phase SPWM Inverter Using Matlab Design and Simulation of a Grid Tied Single Phase SPWM Inverter Using Matlab," 2020, doi: 10.1088/1757-899X/745/1/012009.

[90] J. Ramos-hernanz, J. M. Lopez-guede, and E. Zulueta, "Reverse Saturation Current Analysis in Photovoltaic Cell Models," vol. 12, pp. 231–237, 2017.

[91] S. Modi, "Mathematical Modeling , Simulation and Performance Analysis of Solar Cell,"

2018 Int. Conf. Power Energy, Environ. Intell. Control, pp. 730–734, 2018.

[92] D. C. Huynh and M. W. Dunnigan, "Unknown Parameter Estimation of a Detailed Solar PV Cell Model," 2020, doi: 10.1109/TENCON50793.2020.9293714.

[93] R. Ben Ali, E. Aridhi, and A. Mami, "Design, modeling and simulation of hybrid power system (Photovoltaic-WIND)," *2016 17th Int. Conf. Sci. Tech. Autom. Control Comput. Eng. STA 2016 - Proc.*, pp. 461–467, Jun. 2017, doi: 10.1109/STA.2016.7952008.

[94] T. E. Rao, S. Elango, and G. G. Swamy, "Power management strategy between pv-wind-fuel hybrid system," *Proc. 7th Int. Conf. Electr. Energy Syst. ICEES 2021*, pp. 101–107, Feb. 2021, doi: 10.1109/ICEES51510.2021.9383706.

[95] N. A. Ahmed and M. Miyatake, "A Stand-Alone Hybrid Generation System Combining Solar Photovoltaic and Wind Turbine with Simple Maximum Power Point Tracking Control," pp. 1–7, Feb. 2009, doi: 10.1109/IPEMC.2006.4777984.

[96] K. Anoune, M. Bouya, M. Ghazouani, A. Astito, and A. Ben Abdellah, "Hybrid renewable energy system to maximize the electrical power production," *Proc. 2016 Int. Renew. Sustain. Energy Conf. IRSEC 2016*, pp. 533–539, Jul. 2017, doi: 10.1109/IRSEC.2016.7983992.